Geoelectrical behavior of Miocene and Quaternary strata in eastern Marajó Island/PA

*Lena Simone Barata Souza, IGc-GMG/USP, Brazil
Dilce de Fátima Rossetti, DSR/INPE, Brazil
Vagner Roberto Elis, IAG/USP, Brazil

Abstract

The use of VES in E Marajó Island had discriminated the presence of an interval with anomalous high resistivity, attributed to the presence of the concretionary horizon, this was crucial to define the top of the Barreiras Formation. The lateral occurrence of the Barreiras Fm and the Quaternary deposits and the abrupt passage between these units are consistent with the presence of a tectonic fault. This information supports previous studies that have claimed reactivation along tectonic faults as the responsible for renewing sediment deposition during the Quaternary in island.

1. Introduction

Marajó Island, located at the Amazonas mouth, represents a low lying terrain characterized by great dinamism of its drainage system during the Quaternary. This is revealed by the abundance of morphological features related to paleochannels that are well preserved in the modern landscape, even under the luxuriant forest cover (Rossetti & Valeriano, 2007; Mantelli, 2008).

Vertical electric sounding (VES) have been applied in hydrological studies in Marajó Island since the 1970's, given its good results in this area, the operation facility and the low costs of this geophysical technique (Trancredi, 1972; Kobayashi, 1979; Cavalcanti, 1979; Bezerra, 1979; Porsani, 1981; Gonzáles, 1984; IDESP, 1986; Carrasquila *et al.* 1991). These studies have indicated higher resistivity values (i.e., >1000 Ω.m) in the southern and southeastern portions of the island, in the adjacencies of the towns of Cachoeira do Arari, Ponta de Pedras, Soure and Salvaterra. This was related to the influence of the Miocene Barreiras Formation, which crops out in several localities around these areas. Maximum resistivity values were obtained in iron-bearing concretionary horizon associated with lateritic paleosols that mark the unconformity atop this unit. On the other hand, in the area around Lake Arari, where Quaternary sedimentation dominates, the resistivity recorded up to 100 m depth was much lower, being related to the abundance of muddy lithologies formed during the Holocene evolution of the lake system. This scenario motivates a wider application of VES in Marajó Island aiming the better understanding of the distribution of Miocene and Quaternary deposits. This type of study is highly important, taking into account previous propositions that the distribution of these strata is tectonically controlled (e.g., Rossetti *et al.* 2007). The lack of natural outcrops resulting from the low topographic relief makes the application of geophysical methods, as VES, of great potential to provide information on lithological variations. This type of approach might be useful for helping reconstructing the tectono-sedimentary evolution of Miocene and Quaternary deposits in Marajó Island, as it can reveal terrains that have been tectonically displaced.

The present study presents results obtained from the use of VES in an area located in eastern Marajó Island. The goal is twofolded: 1. to record the spatial distribution of Miocene and Quaternary strata; and 2. to analyse the possible effect of tectonics on this distribution.

2. Material and Methods

This work is based on a total of 21 VES acquired in Marajó Island/PA, next to the localities of Cachoeira do Arari, Salvaterra and Joannes. The acquisition was made by the Schlumberger array method, using a GEOTEST RD-300A resistivemeter, regular exit power of 1000 W, reading interval of 0,1 mV 750 mV, maximum current value of 800 mA, and two 12 V car batteries as source. Cable integrity and the distance between electrodes were carefully controlled during data acquisition. Local noises (iron tubes, electric and/or telephone wiring) were carefully recorded attempting to recognize possible data interference. The electrode distances ranged from 2 m (A/B2=1m) to 640 m (AB/2 = 320 m) (Fig. 2). The flat terrain isolated from antrophic interferences was ideal for undertaken the SEV survey.

3. Results

The results revealed beds with ρ_a varying from 250 to 500 Ωm (sands and iron-bearing sands) that are interbedded with clays and sands displaying ρ_a of 550 and 1500 Ωm, respectively. These deposits grade into mudstones and muddy sands with ρ_a ranging from 0 - 90 Ωm and 95 - 200 Ωm, respectively. Exceptional values > 1500 Ωm are also common, and attributed to lateritic paleosol.

Figure 3 illustrates three of the twenty one soundings modeled in the study area using the program IPI2Win-Geoscan-M Ltd. Five types of deposits, related to mudstone, muddy sand, sand, iron-bearing sand and lateritic concretion, occur in the geoelectric sections A-A', B-B' and C-C', located in the eastern portion of the study area (Fig. 2). The A-A' section (VES 12, 14 and 17; Fig. 4) crosses the area in the W-E direction, perpendicularly to Arari River and parallel to Camará River (Fig. 2). In this section, which is 30 m deep and 7 km long, the lateral continuity of the strata is abruptly interrupted in its median portion. This is recorded by the sudden disappearance of muddy sands overlain by ferruginous sands and lateritic concretions from west to east, which give rise to a muddy unit with local sand lenses.

Section B-B' (Fig. 5) is located in the easternmost portion of the study area, being oriented in the WSW-ENE direction, parallel and perpendicular to the Paracauari and Camará Rivers, respectively (Fig. 2). This section (VES 5, 6, 7, 8, 9, 13, 18 and 19) is characterized by expressive lateral continuity of the lateritic horizon throughout its extension in the first 18 m depth, though thickness is variable from 2 to 20 m. Within this horizon, there are iron-bearing sand lenses 1 to 3 km in length and 0.5 to 4 m thick. In the WSW side of this section (point B), there are isolated sandy bodies close to the surface. To the ENE, there is an isolated lateritic body with 4 km in length and 2 m in thickness is recorded. Alternatively, the high VES value related to laterite concretions could represent limestones, as this lithology is known to occur in surface, being represented by the Amapá Formation. Below 18 m depth, the strata show low lateral continuity, denoting the intercalation of muds, sands and muddy sands up to 140 m depth. Between 18 and 50 m depth, there is an exceptionally continuous iron-bearing sandy body up to 14 km long.

Section C-C' (VES 1, 2, 3 4, 10, 11, 13, 16, 18 and 21; Fig. 6) is located in the eastern portion of the study area, being oriented in the SW-NE direction, perpendicular and parallel to Camará and Paracauari Rivers, respectively (Fig. 2). This section, similar to B-B', displays a lateritic horizon correlatable almost throughout the section, where it presents a thickness of up to 10m. Underlying this horizon, a 14 km long and up to 40 m thick iron-bearing irregular sandy body is recorded. In the extreme SW and NE portions of the section, there are isolated bodies of sand and intercalations of muds and sands. From 10 m up to 80 m depth, the strata are discontinuous, configuring intercalations of muds, muddy sands and sands.

4. Discussion and Conclusion

Vertical electrical sounding is not applicable to distinguish very thin beds. So, the ρ_a value should be taken as an average within a heterogenous sedimentary package. If resistivity is high, one should be aware that the lithology could include, for instance, coarse sand with mud. On the other hand, a low resistive muddy body could display thinner beds of sand and pebbles with high resistivity. Thus, the value ρ_a reflects the material resistivity, the grain size volume and the geometric distribution of the deposit in subsurface.

The previous lithological interpretation (see item 3) is based on the geological context of the region, which is characterized by estuarine massive to stratified sandstones, laminated to massive mudstones and heterolithic sandstones and mudstones of the Barreiras Formation (Arai et al. 1988; Rossetti, 2001). In addition, the area contain Quaternary estuarine and fluvial deposits including mostly muds and sands related to the Post-Barreiras Sediments. The top of the Barreiras Formation is well defined by a discontinuity surface marked by an extensive lateritic paleosol (Rossetti, 2004).

The presence of an interval with anomalous high resistivity, attributed to the presence of the concretionary horizon of lateritic profile, was crucial to define the top of the Barreiras Formation. It is interesting to add that field data corroborate the presence of this paleosol along several points where the VES have indicated high resistivity close to the surface. O geoelectrical model confirms the prevalence of the Barreiras Formation in the Salvaterra area. Therefore, the Miocene deposits become thicker and closer to the surface to the east of the study area. The lateritic paleosol and the underlying deposits of the Barreiras Formation disappear completely westward, being replaced by Quaternary sediments. The absence of lateritic concretions to the west is suggestive of its deeper location below the investigation depth reached by the present VES survey. The lateral occurrence of the Barreiras Formation and the Quaternary deposits in section A-A' and the abrupt passage between these units are consistent with the presence of a tectonic fault. This information supports previous studies that have claimed reactivation along tectonic faults as the responsible for renewing sediment deposition during the Quaternary in Marajó Island (Rossetti et al. 2007; Rossetti et al. 2008).

The good results obtained from the application of VES in eastern Marajó Island lead to propose the continuity of this geophysical method for improving the reconstruction of the tectono-sedimentary history of Miocene and Quaternary deposits in this area. Future studies should include the integration of this technique with the mapping of morphostructural lineaments derived from remote sensing in order to demonstrate the correlation of tectonic faults in surface and sub-surface.

5. Acknowledgements

6. References

Arai, M.; Uesugui, N.; Rossetti, D. F.; Góes, A. M. 1988. Considerações sobre a idade do Grupo Barreiras no nordeste do Estado do Pará. In: Cong. Bras. Geol., 35, Anais....SBG. 2: 738-752.

Bezerra, C. A. 1979. Eletroresistividade aplicada ao estudo de água subterrânea no Município de Salvaterra – Marajó – Pará. Belém (PA). NCGG-UFPA. 58p. (Dissertação de Mestrado).

Carrasquila, A.; Rijo, L; Porsani, M. 1991. Estudo geofísico regional das águas subterrâneas na Island Marajó – Pará. Rev. Bras. Geof., 9 (2): 187-197.

Cavalcanti, G. M. L. 1979. Geofísica aplicada à prospecção de água subterrânea na área do Rio Paracauari – Island Marajó – Pará. Belém (PA). NCGG-UFPA. 88p. (Dissertação de Mestrado).

Gonzáles, A. A. C.1984. Estudo geofísico regional sobre água subterrânea da Island Marajó – Pará – Brasil. Belém (PA). NCGG-UFPA. 143p. (Dissertação de Mestrado).

Instituto de Desenvolvimento Econômico Social do Estado do Pará (IDESP). 1986. Hidrogeologia da Região Oriental da Island Marajó. Belém (PA). Relatório Interno, 97p.

Kobayashi, C. N. 1979. Métodos geofísicos aplicados à prospecção de água subterrânea no Município de Ponta de Pedras. Island Marajó – Pará. Belém (PA). NCGG- UFPA. 93p. (Dissertação de Mestrado).

Mantelli, L. R. 2008. Caracterização geomorfológica no sudoeste da Island Marajó – análise de modelos de elevação digital. São José dos Campos. Sensoriamento Remoto – Instituto Nacional de Pesquisas Espaciais. 70 p. (Dissertação de Mestrado).

Porsani, M. J. 1981. Paleocanais, uma opção para prospecção de água subterrânea na Ilha de Marajó. Belém (PA). NCGG-UFPA. 109p. (Dissertação de Mestrado).

Rossetti, D. F. 2004. Paleosurfaces from northeastern Amazonia as a key for reconstructing paleolandscapes and understanding weathering products. Sedimentary Geology, 169: 151-174.

Rossetti, D. F. 2001. Late Cenozoic sedimentary evolution in northeastern Pará, Brazil, within the context of sea level changes. Journal of South American Earth Sciences, 14: 77-89.

Rossetti, D. F; Góes, A. M.; Valeriano, M. M; Miranda, M. C. C. 2008. Quaternary tectonics in a passive margin: Marajó Island, northern Brazil. Journal of Quaternary Science, 23: 121–135.

Rossetti, D. F. & Valeriano, M. M. 2007. Evolution of the lowest amazon basin modeled from the integration of geological and SRTM topographic data. Catena, 70 (2): 253-265.

Rossetti, D. F.; Valeriano, M. M.; Thallês, M. 2007. An abandoned estuary within Marajó Island: implications for late quaternary paleogeography of northern Brazil. Estuaries and Coasts, v.30, n.5, p.813-826.

Rossetti, D. F., Truckenbrodt, W.; Góes, A. M. 1989. Estudo paleoambiental e estratigráfico dos Sedimentos Barreiras e Pós-Barreiras na região Bragantina, nordeste do Pará. Bol. Museu Paraense Emílio Goeldi, sér. Ciências da Terra 1, 1: 25-28.

Trancredi, A. C. 1972. Aplication de la prospection électrique à l'ètude hidrogéologique da Island Marajó – état du Pará, Bresil. Diplome Et. Sup. Strasbourg, Multig. 25p.
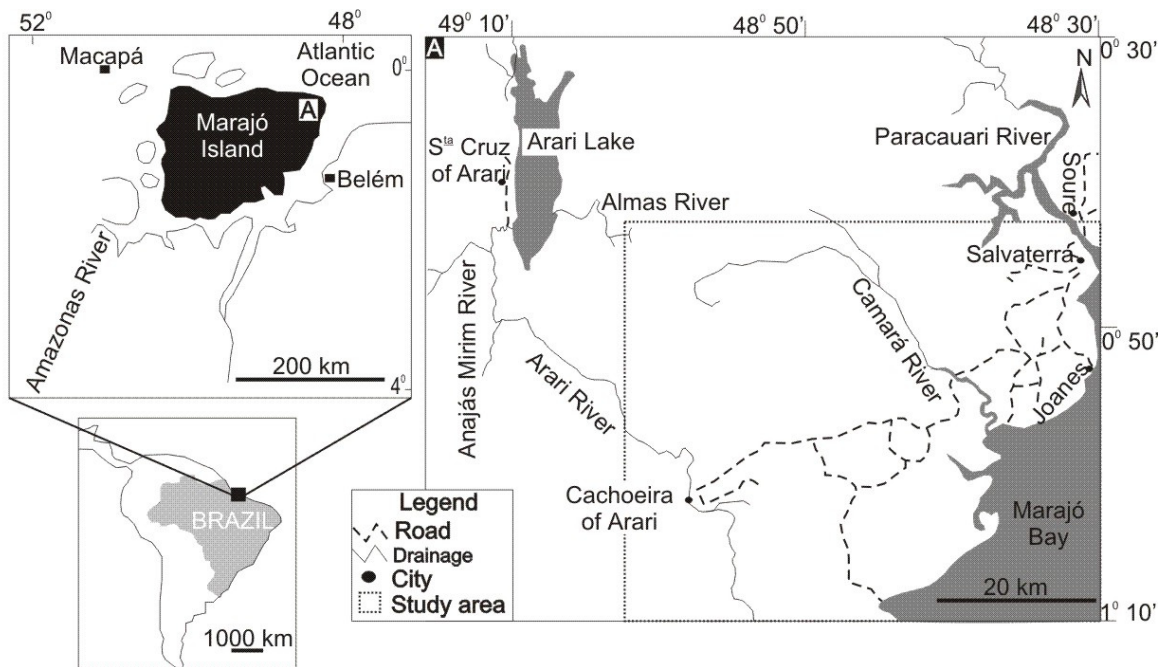
Fig. 1 – Location of the study area in eastern Marajó Island.

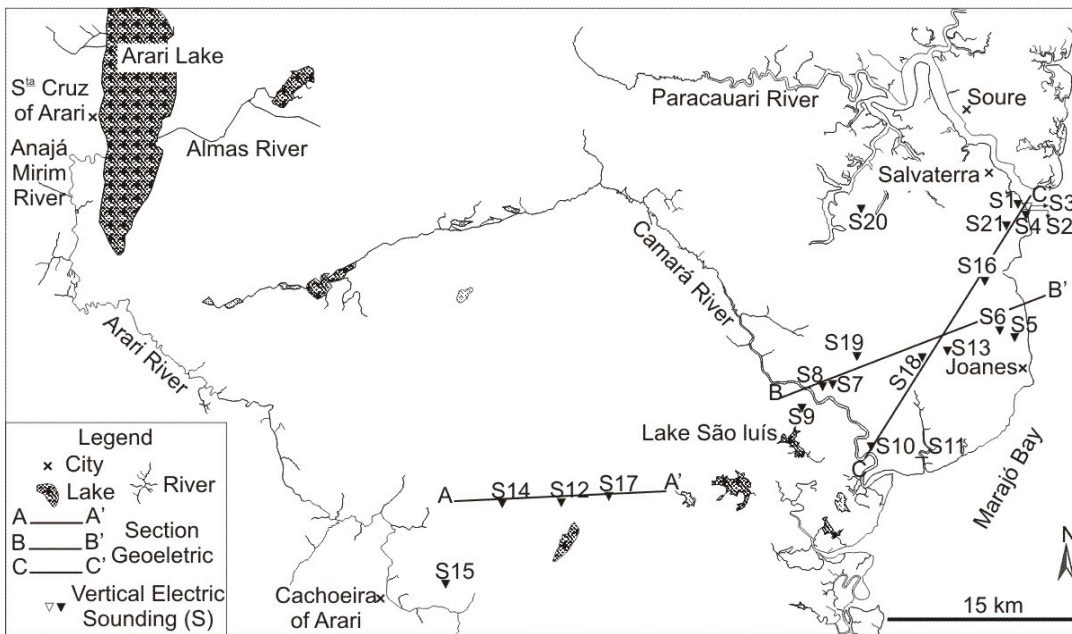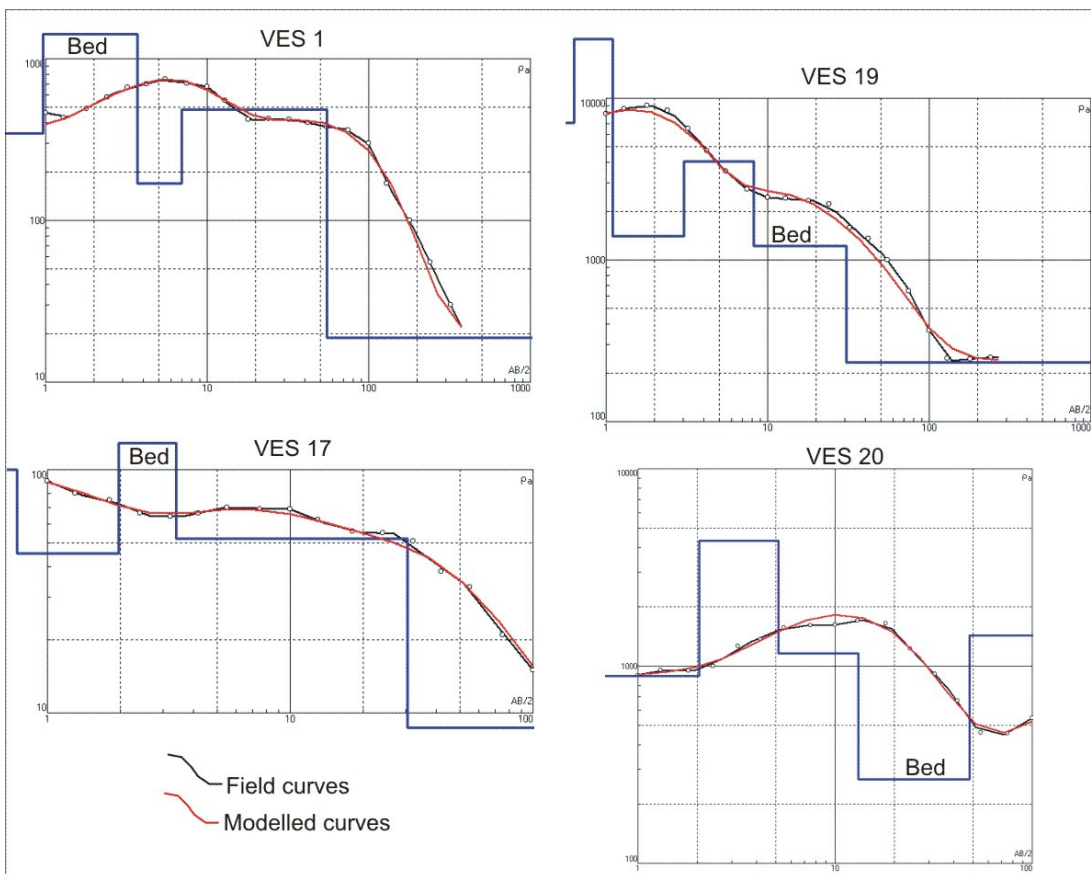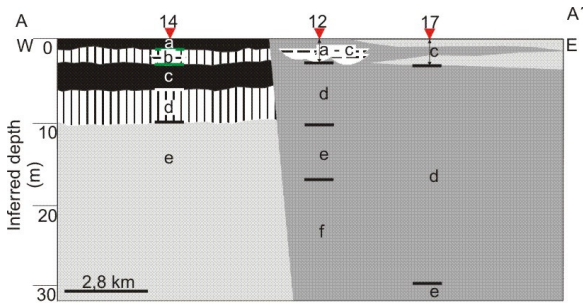Fig. 2 – Location of the VES stations established in the study area.

Fig. 3 – Examples of modelled VES curves for the study area.

	VES12			VES17			VES14		
	ρ (Ωm)	h (m)	d (m)	ρ (Ωm)	h (m)	d (m)	ρ (Ωm)	h (m)	d (m)
a	72,9	0,7	0,7	100	0,8	0,8	2903	1	1
b	379	0,2	0,9	45,2	1,2	2	617	1,6	2,6
c	22,9	2,1	3	129	1,4	3	2728	3,5	6,1
d	64,1	7,3	10,3	52	27	30,4	258	2,8	8,9
e	26	7,4	17,7	8,6	-	-	148	-	-
f	4,6	-	-						

ρ → resistivity; h → thicknesses; d → depth

Legend
Clay Laritic ▼ VES
Sand Fe-bearing sand
Clayey-sand
Limit of valoures of resistivity
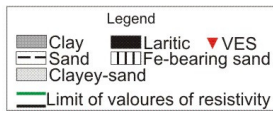
Fig. 4 – Geoelectric section A-A' and lithological interpretation from geophysical data.
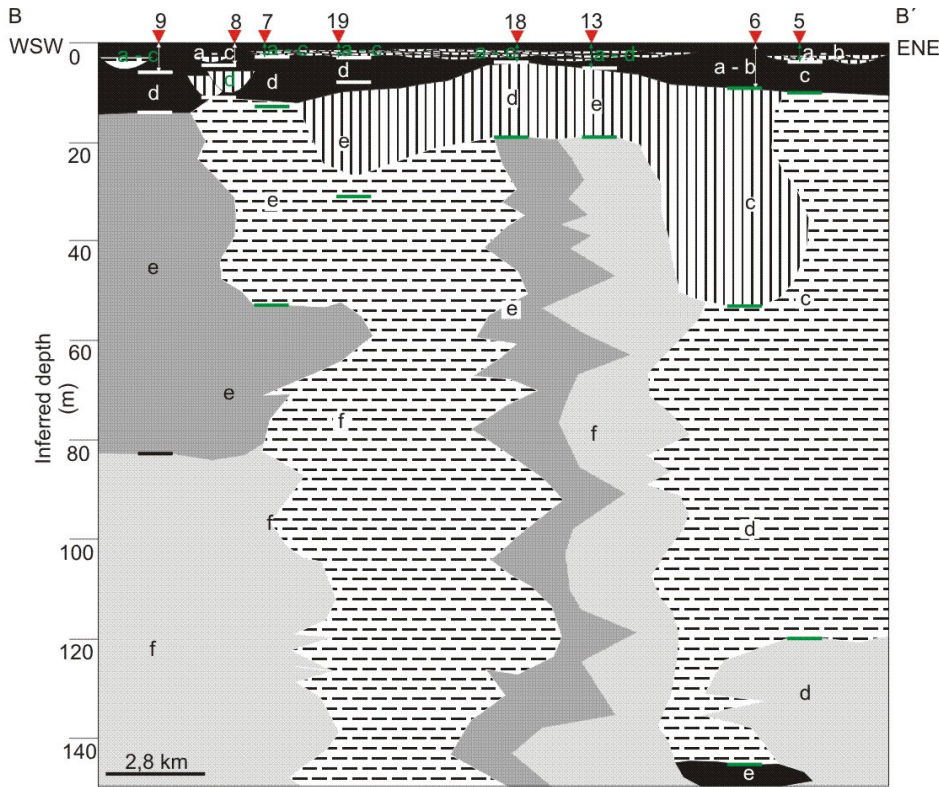
	VES5			VES6			VES7			VES8			VES9			VES13			VES18			VES19		
	ρ (Ωm)	h (m)	d (m)	ρ (Ωm)	h (m)	d (m)	ρ (Ωm)	h (m)	d (m)	ρ (Ωm)	h (m)	d (m)	ρ (Ωm)	h (m)	d (m)	ρ (Ωm)	h (m)	d (m)	ρ (Ωm)	h (m)	d (m)	ρ (Ωm)	h (m)	d (m)
a	7862	2,2	2,2	6831	2,3	2,3	2721	0,3	0,3	1444	0,5	0,5	10169	1,3	1,3	3452	0,6	0,6	2335	0,7	0,7	7043	0,6	0,6
b	1316	2,4	4,7	2609	7,2	9,6	10112	0,8	1,1	663	0,8	1,4	2178	3,3	4,6	9544	0,4	1,1	1036	0,5	1,3	23201	0,5	1,1
c	6811	6,2	10,9	1113	44,2	53,8	1000	2,1	3,2	2278	8,3	9,7	581	2,1	6,8	1523	0,8	1,9	2040	1,8	3	1404	1,9	3
d	388	103	114	417	91	145	3438	10,1	13,3	831	13,9	23,6	1560	7,9	14,8	2214	2,1	4,5	943	14,9	17,9	4066	5,2	8,2
e	125	-	-	3059	-	-	421	40,3	53,6	35,5	-	-	72,4	68,9	83,7	1060	12,4	16,9	73,8	-	-	1220	22,5	30,7
f							53,6	-	-				132	-	-	137	-	-				232	-	-

ρ → resistivity; h → thicknesses; d → depth

Legend
Clay Laritic ▼ VES
Sand Fe-bearing sand
Clayey-sand
Limit of valoures of resistivity

Fig. 5 – Geoelectric section B-B' and lithological interpretation from geophysical data.

	VES1 ρ (Ωm)	h (m)	d (m)	VES2 ρ (Ωm)	h (m)	d (m)	VES3 ρ (Ωm)	h (m)	d (m)	VES4 ρ (Ωm)	h (m)	d (m)	VES10 ρ (Ωm)	h (m)	d (m)	VES11 ρ (Ωm)	h (m)	d (m)	VES13 ρ (Ωm)	h (m)	d (m)	VES16 ρ (Ωm)	h (m)	d (m)
a	347	0,9	0,9	2845	0,8	0,8	1113	0,6	0,6	1559	0,7	0,7	701	0,3	0,3	770	0,5	0,5	3452	0,6	0,6	3372	0,7	0,7
b	1418	2,7	3,7	819	2,5	3,4	1721	5,4	6	2542	8,3	9	1015	0,6	0,9	1792	2,8	3,4	9544	0,4	1,1	12057	1	1,7
c	169	3,2	6,9	3800	3,5	7	530	79,3	85,4	371	22,1	31,1	656	4,4	5,2	227	3,9	7,3	1523	0,8	1,9	2403	5,2	6,8
d	484	48,4	55,4	109	21,1	28,1	0,7	-	-	176	-	-	211	3,1	8,4	20,2	15	22,3	2214	2,1	4,5	943	23,5	30,4
e	18,7	-	-	60,6	-	-							14,4	-	-	40,6	-	-	1060	12,4	16,9	290	-	-
f																			137	-	-			

	VES18 ρ (Ωm)	h (m)	d (m)	VES21 ρ (Ωm)	h (m)	d (m)
a	2335	0,7	0,7	3412	0,8	0,8
b	1036	0,5	1,3	7824	1,2	2
c	2040	1,8	3	1471	4,6	6,6
d	943	14,9	17,9	564	5,6	12,2
e	73,8	-	-	1387	27,1	39,3
f				571	-	-

ρ → resistivity; h → thicknesses; d → depth

Legend

Clay   Laritic   ▼ VES
Sand   Fe-bearing sand
Clayey-sand
Limit of valoures of resistivity

Fig. 6 – Geoelectric section C-C' and lithological interpretation from geophysical data.